Desalination and Water Treatment
www.deswater.com

doi: 10.5004/dwt.2021.26788

211 (2021) 448–455
January

Nutrient recovery from concentrated municipal wastewater by forward osmosis membrane and $MgCl_2$ based draw solution

Mohammad Damirchi[a,b], Ismail Koyuncu[a,b,*]

[a]*National Research Center on Membrane Technologies, Istanbul Technical University, Maslak 34469, Istanbul, Turkey, emails: Koyuncu@itu.edu.tr (I. Koyuncu), damirchi15@itu.edu.tr (M. Damirchi)*
[b]*Istanbul Technical University, Environmental Engineering Department, Maslak 34469, Istanbul, Turkey*

Received 11 February 2020; Accepted 12 November 2020

ABSTRACT

In this study, a forward osmosis membrane was used to concentrate municipal wastewater up to 90%. The concentrated wastewater provided a high content organic matter for subsequent anaerobic treatment. At the same time, phosphorus content was recovered via precipitation. Energy-dispersive X-ray spectroscopy was done to evaluate the recovered solid. Results showed that precipitated phosphorus constituted only 2.46% cellulose triacetate (CTA membrane) and 2.24% thin-film composite (TFC membrane) of the total recovered solid. Although these percentages account for 72% of total phosphorus in the CTA test and 56% of total phosphorus in the TFC test, recovery of unwanted precipitate (Calcite) is still the main drawback. This can be attributed to the high calcium to phosphorus molar ratio in municipal wastewater and the presence of bicarbonate, which ultimately facilitates the formation of calcite as the dominant recovered solid. Regardless of membrane type, complete water flux recovery was achieved after chemical cleaning. It indicates that chemical cleaning can effectively recover the water flux to its virgin membrane flux for direct municipal wastewater concentration.

Keywords: Forward osmosis; Municipal wastewater; Magnesium chloride; Calcite; Phosphorus

1. Introduction

Municipal wastewater has been widely accepted as one of the emerging sources for the recovery of nutrients [1] and harvesting energy [2]. With respect to nutrient, attentions have been drawn to exploit recoverable phosphorus in municipal and industrial wastewater. Theoretically, P load in municipal wastewater can replace 40% to 50% of applied mineral P fertilizer in agriculture [3].

Regarding the energy recovery, due to low carbon matter in municipal wastewater and given the fact that the yield of biogas production is proportional to chemical oxygen demand (COD) of feed solution in the anaerobic process [4], the challenging issue is how to have an efficient and stable anaerobic process. To tackle this, pre-concentration of wastewater can significantly boost the performance of anaerobic treatment through increasing the carbon content entering the reactor and reducing the amount of solubilized methane in the effluent stream [5]. Direct membrane filtration concept including pressure-driven, osmosis-driven, thermal-driven, electrical-driven has gained great attention, while little has known about factors affecting costs and benefits of each of these technologies.

Forward osmosis (FO) is a non-pressure-driven membrane separation process in which water passes across a semi-permeable membrane from a low-osmotic-pressure (feed solution) side to a high-osmotic-pressure (draw solution) [6–8]. Given the fact that no hydraulic pressure is

* Corresponding author.

Presented at the 6th MEMTEK International Symposium on Membrane Technologies and Applications (MEMTEK 2019), 18–20 November 2019, Istanbul, Turkey

used in the FO process to extract water, it has low energy consumption [9]. High water quality, high rejection of pollutants and better fouling reversibility in comparison with pressure-driven reverse osmosis membrane filtration [10] are other advantages of this process. These characteristics enable FO to concentrate various streams such as activated sludge [11,12], urine [13,14], raw sewage [9,15–17]. It is possible to take advantage of the reverse solute diffusion phenomenon to supply required cation for nutrient recovery in form of struvite or other precipitates. In this way, magnesium-based draw solution can provide osmotic pressure as the driving force of forward osmosis as well as the required magnesium to form the precipitate [18–20]. Diffusion of a hydrogen ion from feed solution to draw solution occurs to keep the electroneutrality [21]. This natural phenomenon facilitates to increase in the pH of the solution which is substantial for phosphate-containing precipitates [19].

Two common types of the membrane were used in this study. Cellulose triacetate (CTA) membrane Hydration Technology Innovations (HTI, Albany, OR) is highly resistant to chlorine and thin-film composite (TFC) membrane which is superior to CTA membrane in terms of permeability and stability at wider pH ranges. Compared to the CTA membrane, an active layer of TFC polyamide membranes (HTI) was formed with lower contact angles to increase biofouling resistance [22].

To the best of our knowledge, most researches have been focused on the use of FO in order to increase the organic content of wastewater and little is known about the possibility of P recovery prior to any anaerobic process. So, the objective of this study was to investigate the concentration of real sewage by FO and using $MgCl_2$ as a draw solution. Water flux, changes in the concentration of ions in feed solution and pH variation were examined at different water recovery percentages. Moreover, the potential of precipitate formation without any chemical addition was studied.

2. Materials and methods

2.1. Forward osmosis system

The forward osmosis system was consisted of a draw solution tank, a feed solution tank and an external membrane module with an effective membrane area of 40 cm^2 and depth of 2 mm. A CTA-ES membrane with embedded polyester screen support with pure water permeability constant of 0.857 L/m^2 h bar and solute permeability constant of 0.259 L/m^2 h a TFC-ES membrane with embedded polyester screen support with pure water permeability constant of 1.470 L/m^2 h bar and solute permeability constant of 0.622 L/m^2 h were acquired from Hydration Technology Innovations (HTI, Albany, OR) and were installed with the active layer of the membrane facing the feed solution. In the beginning, 3 L of 0.5 M magnesium chloride was used as draw solution and its tank was placed on an electronic balance which was connected to a computer to record the weight changes for following water flux calculation. A conductivity meter was placed in the feed tank to monitor the salinity change, while a potable pH probe recorded the possible pH variation. Due to dilution of draw solution through the time, another 4 molar $MgCl_2$ reservoir was used to add $MgCl_2$ automatically to the DS tank, in order to work under constant osmotic pressure. The flow rate of 1 l/min was adjusted for recirculation of both feed and draw solution, corresponding to the cross-flow velocity of 16.7 cm/s.

Primary effluent (i.e., wastewater after primary sedimentation) was obtained from Pashakoy Wastewater Treatment Plant. This wastewater was first filtered by a coarse filter in the laboratory prior to being used as a feed solution. The physicochemical characteristics of the feed are summarized in Table 1.

2.2. Analytical methods

COD was measured using a Hach DRB200 COD Reactor and Hach DR5000 spectrophotometer. Ammonia nitrogen (NH_4^+–N), orthophosphate (PO_4^{-3}–P) and total suspended solids (TSS) of untreated wastewater and concentrated wastewater at different water recoveries were measured according to Standard Methods for the Examination of Water and Wastewater. All metallic cations (Mg^{2+}, Ca^{2+}, K^+, Na^+) and anions (Cl^-, SO_4^{2-}) were measured by ion chromatography (Dionex ICS3000). Water flux (LMH) was calculated through the whole experiment by measuring the change in weight of the draw solution and dividing it by surface membrane area and time duration. The morphology and composition of precipitants were analyzed by using scanning electron microscopy coupled with energy-dispersive X-ray spectroscopy (SEM-EDX). Samples were coated with platinum/palladium prior to analysis.

2.3. Membrane cleaning protocol

Both physical and chemical cleaning was done after the wastewater concentration and water flux was measured after each step. For both the feed side and draw side, in-situ physical cleaning was applied by using tap water to remove a portion of the fouling layer formed on the membrane surface. A two-step chemical cleaning protocol [23] was used for both sides of the membrane. 0.1% NaOH/0.1% SDS mixture was recirculated with a cross-flow velocity of 20 cm/s for 30 min, followed by acid cleaning with 2% citric acid for another 30 min at the same cross-flow velocity.

Table 1
Physicochemical characteristics of filtered primary effluent wastewater

Parameters	Values (CTA test)	Values (TFC test)
Total chemical oxygen demand, mg/L	258	275
Total suspended solids, mg/L	85	95
Ammonium, mg/L	41.18	33.11
Orthophosphate (PO_4^{3-}–P), mg/L	6.16	4.61
Ca^{2+}, mg/L	60.56	65.99
SO_4^{2-}, mg/L	83.26	88.76
Mg^{2+}, mg/L	12.85	13.44
pH	7.25	7.49
Conductivity, mS/cm	1.503	1.273

For each step and also at the end of the cleaning campaign, the membrane was slowly washed with distilled water.

2.4. Potential precipitates

In order to find out potential precipitation in the feed solution, Visual MINTEQ (v. 3.1) was used to model the chemical equilibrium and to calculate the supersaturation index (SI). The input data was based on ion measurements on different water recovery percentages.

3. Results and discussions

3.1. Water flux and fouling behavior

Experiments were carried out for both CTA and TFC membranes to reach 90% water recovery and a total of 3.6 L of water was extracted. Using 0.5 M $MgCl_2$ as draw solution through both experiments, the osmotic pressure of draw solution was fixed by the addition of a secondary high concentration stream from the reservoir tank. Thus, the observed water flux decline was likely caused by membrane fouling and the elevated osmotic pressure of feed solution [16]. The latter was due to both reverse salt flux and concentrated feed solution. Flux was steadily decreased from 10.05 to 6.52 LMH at 50% water recovery. As can be seen from Fig. 1, further water recovery contributed to a severe decline in flux between 65% (6.10 LMH) to 90% (3.20 LMH) water recovery for the CTA membrane. A similar decline can be seen for TFC where water flux was 5.85 LMH (at 50%) decaling to 3.68 LMH at 90% water recovery.

Regardless of membrane types, this can be explained by the accumulation of salt in feed solution which leads to loss of osmotic pressure gradient as the driving force and formation of cake layer which enhance the cake enhance concentration polarization (CECP). Wang et al. [24] have suggested that the reverse solute flux dominated the decrease of water flux during the concentrating process, while the CECP and ECP contributions were similar. In the current experiment, when water flux at the end of the experiment subtracted from the water flux of the fouled membrane measured by distilled water, it shows a 41% and 34% water flux decline due to reverse solute for CTA and TFC, respectively. Another explanation for the sharp decline in water flux may be due to the formation of precipitates namely calcium carbonate and calcium phosphate on membrane surface reported by [25,26]. Our finding also corroborated the role of scaling in flux decline as precipitated compounds were mainly composed of $CaCO_3$ in the current study.

At the end of the batch test, fresh draw solution and deionized water were used to evaluate the membrane fouling. Fig. 2 summarizes water flux recovery after each cleaning step. Fouled membrane flux was 7.35LMH and 7.25 LMH for CTA and TFC respectively, accounting for 72% and 69% of virgin membrane flux. Since DI water was used here, the share of reverse solute in total fouling was deducted, so it can be concluded that for CTA membrane, 28% of fouling was associated with the formation of the cake layer, while in the case of TFC membrane it was 31%. The membrane surface was flushed with tap water to examine the effect of physical cleaning. Water flux reached 9.7 LMH for CTA which equals 96% of virgin membrane flux. This high flux recovery can prove the high reversibility characteristic of the FO membrane which is in accordance with previous studies [17,27]. Regardless of membrane type, complete water flux recovery was achieved after chemical cleaning. It indicates that chemical cleaning can effectively recover the water flux to its virgin membrane flux for direct municipal wastewater concentration.

3.2. Nutrient concentration and ions rejection by FO membrane

Depending on the type of pollutant and membrane materials, different rejection rates were achieved. High concentrating efficiency was obtained for ortho-phosphate (always below the detection limit in the draw tank) for both the CTA and TFC membrane. While removal efficiency of ammonium in TFC was only 25.6% (at CF = 10), in the case of CTA one, this number reached to 34% at the same concentration factor of 10. This is likely due to higher ammonium permeability in the TFC membrane compared to the CTA type. In the case of CTA, the ammonium concentration increased from 41.18 to 140.21 mg/L, resulting in a decrease of ammonium concentration factor to wastewater concentration factor ratio from 1 to 0.34. As can be seen from Fig. 3, this ratio declined to 0.26 for the TFC one.

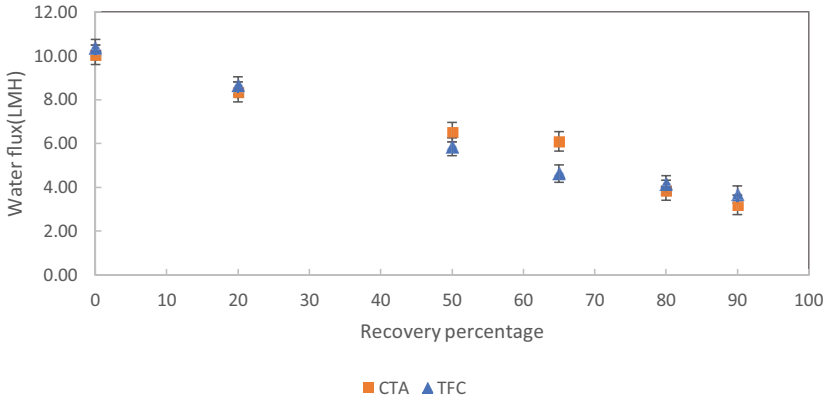

Fig. 1. Variation of water flux during wastewater pre-concentration by CTA and TFC membrane (4 L sewage as initial feed solution and 0.5 molar $MgCl_2$ as draw solution).

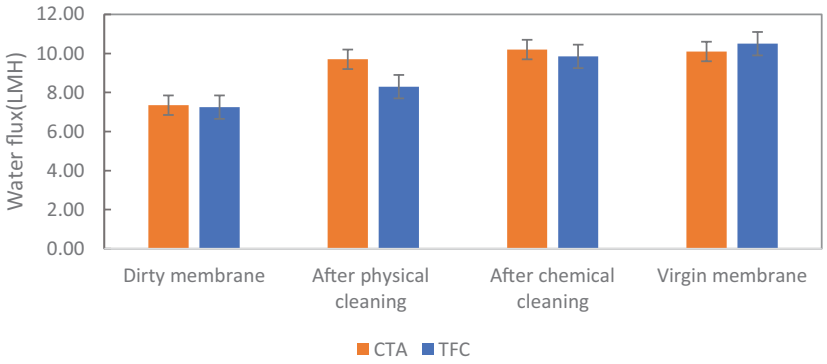

Fig. 2. Water flux for fouled membrane using distilled water at the end of sewage concentration and recovered flux after each membrane cleaning step.

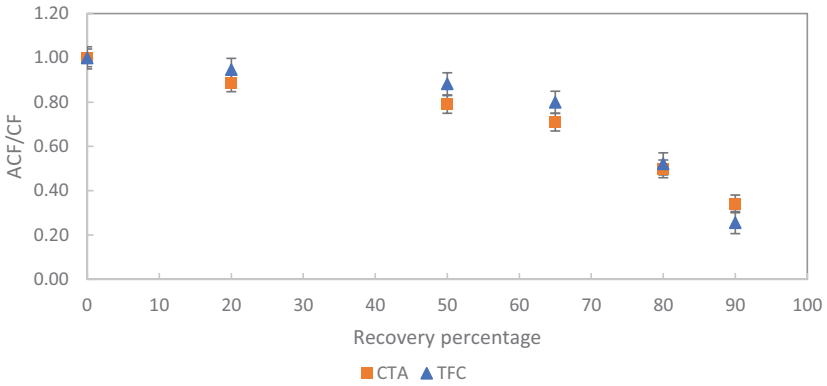

Fig. 3. Ammonium concentration factor to sewage concentration factor ratio in CTA and TFC membranes.

From 65% to 90% water recovery, the performance of the TFC membrane in rejection of ammonium was more deteriorated compared to CTA one, whereas up to 65% water recovery, TFC showed slightly better rejection capability. Lack of CTA and TFC membrane in rejection of this pollutant, confirming the bidirectional diffusion of NH_4^+ [28] and is in line with findings of [24] reported only 48% rejection of ammonium. Since the draw solution concentration was constant through the experiment, it can be concluded that NH_4^+ flux is proportional to its initial concentration. Concerning any potential ammonium containing recovered nutrients, 65% water recovery can be considered as the maximum concentration factor in order to not to lose NH_4^+.

Regardless of membrane type, high performance in rejecting the phosphate is associated with two mechanisms. Firstly, the negative charge of the membrane surface can repulse the phosphate ions via electrostatic repulsion. Secondly, since phosphate has a large hydrated radius, size exclusion can hinder it to pass through the membrane pores.

As can be seen from Fig. 4, in the case of CTA membrane, orthophosphate concentration in feed solution slightly increased until 50% water recovery, although, at this point, its concentration factor was still much lower than wastewater concentration factor. Regardless of membrane type, given the fact that phosphate was absence in the draw solution, it can be concluded that a portion of orthophosphate was likely transformed to other forms ($MgHPO_4$ and $CaHPO_4$), precipitated or physically was adsorbed to other particles. With further the filtration time, phosphate removal/precipitation from feed solution bulk was reached to 92.53% and 86.46% for CTA and TFC, respectively. Analysis of precipitation by SEM-EDX proved the presence of phosphorus in solid which have been discussed in detail in the following section. Regarding calcium and sulfate, these ions can be retained completely by the FO membrane.

Illustrating in Fig. 5, it can be observed that as the total content of Ca^{2+} and SO_4^{2-} until 80% water recovery was not changed, implying that these ions didn't participate in any physicochemical reactions, more water recovery can facilitate the reaction of Ca^{2+} and Mg^{2+} with sulfate. High rejection of sulfate alongside with the decrease of total sulfate in feed solution from 80% to 90% water recovery can prove that a portion of calcium and magnesium are likely to react with sulfate to form magnesium sulfate and calcium sulfate.

Comparing the distribution species of sulfate at 80% and 90% water recoveries by Visual MINTEQ corroborates this claim, where the distribution of $MgSO_4$ increased from 29.61% to 38.47%, for TFC membrane while in the case of CTA, $MgSO_4$ distribution raised from 14.35% to 27.50%. Concerning COD, results show that FO can effectively concentrate the wastewater up to fivefold, from 258 to 1,319 mg/L for the CTA membrane and up to 7-fold for the TFC membrane increasing from 275 to 2,053 mg/L. It is noteworthy that lower than expected CF can be explained by attachment of organic matter to the membrane surface, forming the cake layer and also as a result of long operating

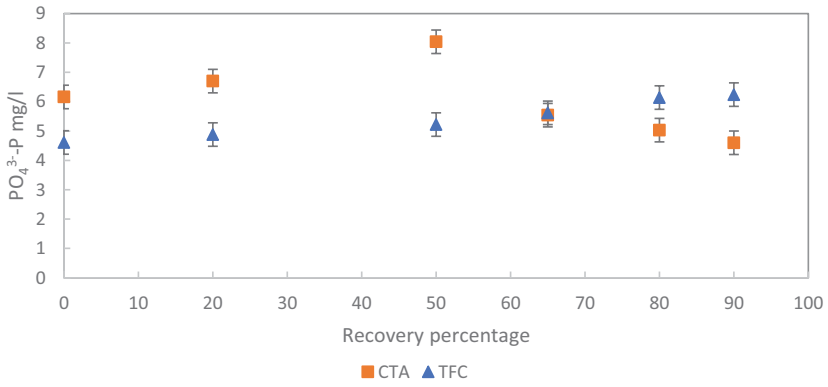

Fig. 4. Variation of orthophosphate concentration during wastewater pre-concentration in the bulk of feed solution.

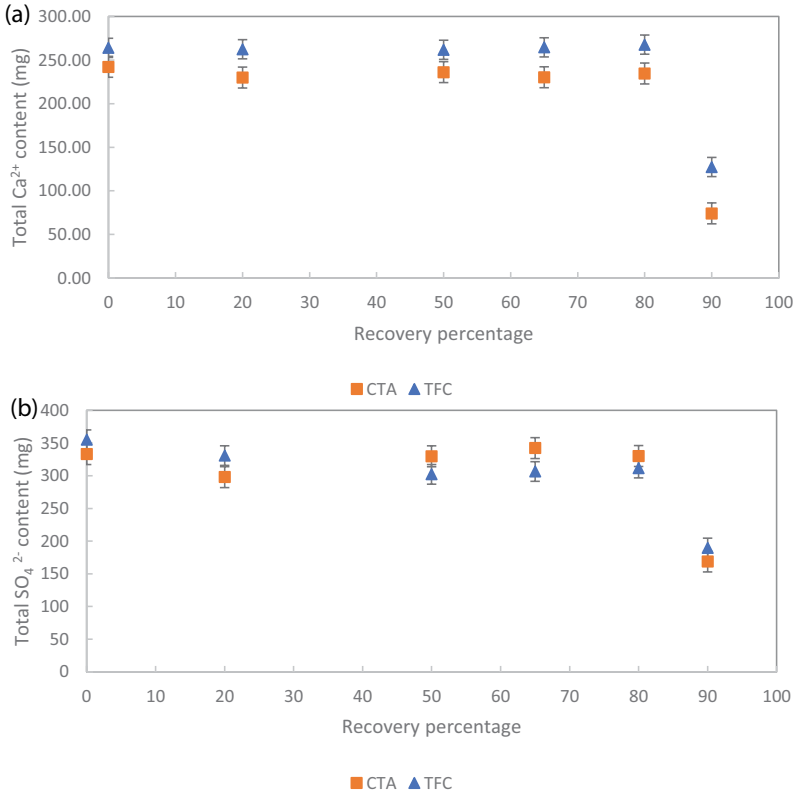

Fig. 5. The total content of (a) Ca^{2+} and (b) SO_4^{2-} in feed solution bulk during wastewater pre-concentration.

time of experiment which makes the biodegradation of organic matter possible. While higher COD values would be beneficial for the subsequent anaerobic processes, salinity accumulation can be detrimental for microorganisms. An increase in salinity is associated with the high rejection capability of FO membrane and reverse diffusion of solute from draw solution to feed solution. These two factors reduce the effective osmotic driving force which is substantial for stable water flux.

Feed conductivity increased from 1.5 to 10.06 mS/cm in the CTA experiment. As mentioned before, $MgCl_2$ was used as a draw solution, so both chloride and magnesium diffuse through the support layer and active layer to the feed side. The value of the hydrated diameter ion of Mg^{2+} and Cl^- are 0.8 and 0.3 nm, respectively, resulting in diffusion constants of 0.55×10^{-9} m²/s for Mg^{2+} ion and 1.5×10^{-9} m²/s for Cl^- ion. Due to this lower diffusion coefficient of divalent ions compared to monovalent ions [29], chloride diffuses easier. Assuming no physicochemical reaction from the beginning of test until 20% water recovery, for CTA membrane, the calculated RSF of Mg^{2+} was 0.188 g/h m² whereas RSF of Cl^- was 1.35 g/h m² while in the case of TFC, RSF of Mg^{2+} and Cl^- were 1.148 and 4.56 g/h m², respectively.

3.3. Recovered solids

To clarify the content of the obtained precipitate, SEM was carried out after 90% water recovery. SEM image

(Fig. 6) confirmed the presence of calcium carbonate as the dominant recovered solid for both membrane types. Specifically, the trigonal morphology reveals the formation of calcite. An EDX was also used to quantify the elemental composition of precipitates. A high percentage of calcium, carbon and oxygen in recovered solids measured by EDX analysis (Fig. 7) corroborates this matter. Although using Visual MINTEQ to calculate supersaturation index (Table S1) suggests the precipitation of P as hydroxyapatite (HAP) and amorphous calcium phosphate (ACP), the presence of organic matter and inorganic carbon facilitates the formation of other precipitates. In fact, the Ca^{2+}/P molar ratio in the current test was always above 5 which is more than required for P precipitation. Therefore, P consumes only a small fraction of Ca^{2+} in feed solution and this provides a suitable condition for (bi) carbonate and calcium to form calcite. This was corroborated by [30], applying electrolysis to extract phosphorus from municipal wastewater.

A rough calculation by using TSS (1,805 mg/L for CTA and 1,390 mg/L for TFC) at 90% water recovery as a solid part of the solution and phosphorus content of recovered solid (2.46 wt.% in the case of CTA and 2.24 wt.% in the case of TFC indicates that 72% of total phosphorus recovered in the form of precipitated phosphorus, while only 56% of total P precipitated in the case of TFC. Relatively lower recovered P in TFC experiment compared to CTA one can be associated with shorter time to reach 90% water recovery in TFC experiment, implying the importance of mixing time required for higher P recovery. Mg^{2+} concentration increased due to RSF in feed solution and Mg^{2+}/Ca^{2+} molar ratio exceeded 1 at 65% water recovery for CTA membrane while this ratio was above 1 from the beginning for TFC membrane, expecting the formation of $Mg(OH)_2$, $Mg_2(OH)_3Cl{\cdot}4H_2O$, $Mg_3(PO_4)_2$ or struvite, however, the thermodynamic calculation (SI < 0, Table S1) and low amount of magnesium (0.98 wt.% for CTA and 1.08 wt.% for TFC) in recovered solid proved the infeasibility of their formations.

4. Conclusions

In this study, it was proved that forward osmosis can effectively concentrate the municipal wastewater, forming a higher COD content stream for the subsequent anaerobic processes. Prior to this step, elevated pH in feed solution together with high rejection of FO provides an opportunity to recover phosphorus by precipitation. Although 72% of phosphorus in the CTA test and 56% of phosphorus in the TFC test were recovered as solid, recovery of unwanted precipitate (Calcite) is still the main drawback in achieving this goal due to low P content of municipal wastewater and its

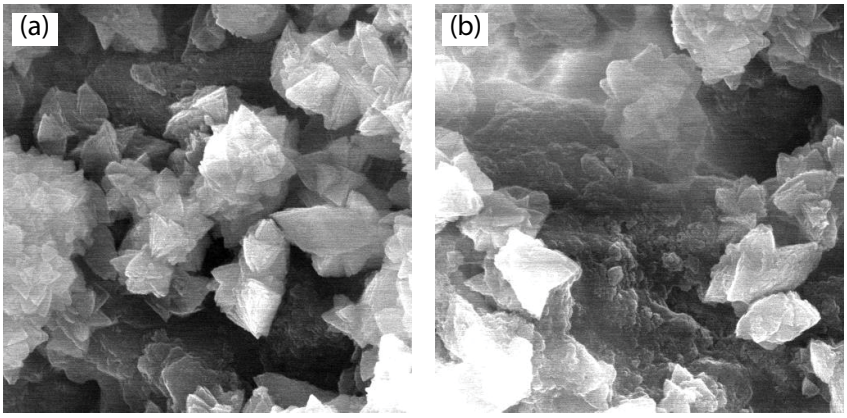

Fig. 6. Scanning electron microscopic images of recovered solids: (a) CTA and (b) TFC experiment.

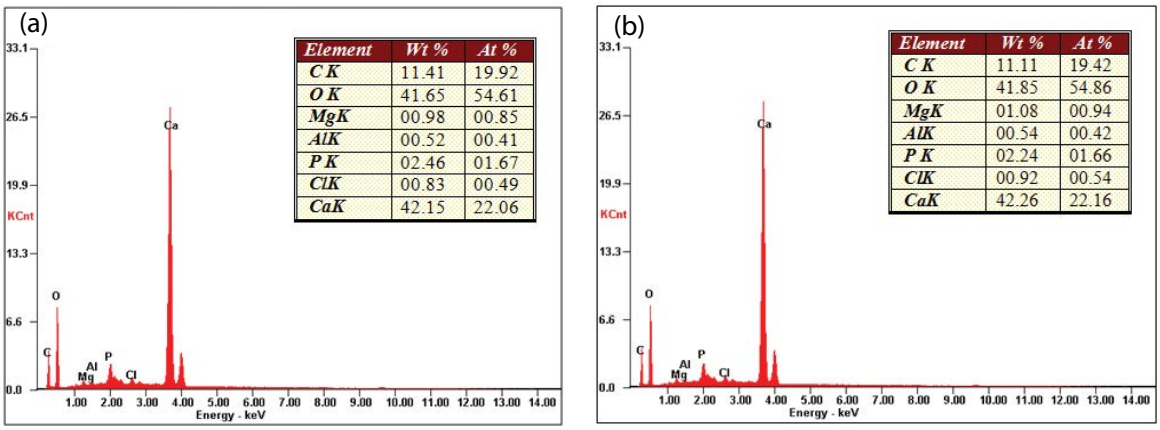

Fig. 7. Energy-dispersive X-ray spectrometry and elemental composition of precipitates: (a) CTA and (b) TFC experiment.

complex nature. Further research is required to find ways for selective precipitation phosphorus and to achieve this goal, the role of (bi) carbonate as the major contributor of calcium carbonate formation should be considered.

References

[1] L.E. de-Bashan, Y. Bashan, Recent advances in removing phosphorus from wastewater and its future use as fertilizer (1997–2003), Water Res., 38 (2004) 4222–4246.

[2] H. Ozgun, R.K. Dereli, M.E. Ersahin, C. Kinaci, H. Spanjers, J.B. van Lier, A review of anaerobic membrane bioreactors for municipal wastewater treatment: integration options, limitations and expectations, Sep. Purif. Technol., 118 (2013) 89–104.

[3] L. Egle, H. Rechberger, J. Krampe, M. Zessner, Phosphorus recovery from municipal wastewater: an integrated comparative technological, environmental and economic assessment of P recovery technologies, Sci. Total Environ., 571 (2016) 522–542.

[4] A.J. Ansari, F.I. Hai, W.E. Price, J.E. Drewes, L.D. Nghiem, Forward osmosis as a platform for resource recovery from municipal wastewater - a critical assessment of the literature, J. Membr. Sci., 529 (2017) 195–206.

[5] A.L. Smith, L.B. Stadler, N.G. Love, S.J. Skerlos, L. Raskin, Perspectives on anaerobic membrane bioreactor treatment of domestic wastewater: a critical review, Bioresour. Technol., 122 (2012) 149–159.

[6] Y. Xu, L. Zhou, Q. Jia, Nutrient recovery of source-separated urine via forward osmosis and a pilot-scale resource-oriented sanitation system, Desal. Water Treat., 91 (2017) 252–259.

[7] M. Xie, H.K. Shon, S.R. Gray, M. Elimelech, Membrane-based processes for wastewater nutrient recovery: technology, challenges, and future direction, Water Res., 89 (2016) 210–221.

[8] S. Subramani, R.C. Panda, B. Panda, Studies on performances of membrane, draw solute and modeling of forward osmosis process in desalination – a review, Desal. Water Treat., 70 (2017) 46–63.

[9] A.J. Ansari, F.I. Hai, W.S. Guo, H.H. Ngo, W.E. Price, L.D. Nghiem, Factors governing the pre-concentration of wastewater using forward osmosis for subsequent resource recovery, Sci. Total Environ., 566–567 (2016) 559–566.

[10] S.Y. Lee, C.H. Boo, M. Elimelech, S.K. Hong, Comparison of fouling behavior in forward osmosis (FO) and reverse osmosis (RO), J. Membr. Sci., 365 (2010) 34–39.

[11] N.C. Nguyen, S.S. Chen, H.Y. Yang, N.T. Hau, Application of forward osmosis on dewatering of high nutrient sludge, Bioresour. Technol., 132 (2013) 224–229.

[12] N.T. Hau, S.S. Chen, N.C. Nguyen, K.Z. Huang, H.H. Ngo, W. Guo, Exploration of EDTA sodium salt as novel draw solution in forward osmosis process for dewatering of high nutrient sludge, J. Membr. Sci., 455 (2014) 305–311.

[13] J.F. Zhang, Q.H. She, V.W.C. Chang, C.Y. Tang, R.D. Webster, Mining nutrients (N, K, P) from urban source-separated urine by forward osmosis dewatering, Environ. Sci. Technol., 48 (2014) 3386–3394.

[14] F. Volpin, H. Heo, M.A. Hasan Johir, J. Cho, S. Phuntsho, H.K. Shon, Techno-economic feasibility of recovering phosphorus, nitrogen and water from dilute human urine via forward osmosis, Water Res., 150 (2019) 47–55.

[15] T.Y. Cath, S. Gormly, E.G. Beaudry, M.T. Flynn, V.D. Adams, A.E. Childress, Membrane contactor processes for wastewater reclamation in space: Part I. Direct osmotic concentration as pretreatment for reverse osmosis, J. Membr. Sci., 257 (2005) 85–98.

[16] X.W. Zhang, Z.Y. Ning, D.K. Wang, J.C. Diniz da Costa, Processing municipal wastewaters by forward osmosis using CTA membrane, J. Membr. Sci., 468 (2014) 269–275.

[17] Y. Gao, Z. Fang, P. Liang, X. Huang, Direct concentration of municipal sewage by forward osmosis and membrane fouling behavior, Bioresour. Technol., 247 (2018) 730–735.

[18] G.L. Qiu, Y.-P. Ting, Direct phosphorus recovery from municipal wastewater via osmotic membrane bioreactor (OMBR) for wastewater treatment, Bioresour. Technol., 170 (2014) 221–229.

[19] M. Xie, L.D. Nghiem, W.E. Price, M. Elimelech, Toward resource recovery from wastewater: extraction of phosphorus from digested sludge using a hybrid forward osmosis-membrane distillation process, Environ. Sci. Technol. Lett., 1 (2014) 191–195.

[20] Z.Y. Wu, S.Q. Zou, B. Zhang, L.J. Wang, Z. He, Forward *in-situ* osmosis promoted formation of struvite with simultaneous water recovery from digested swine wastewater, Chem. Eng. J., 342 (2018) 274–280.

[21] N.T. Hancock, W.A. Phillip, M. Elimelech, T.Y. Cath, Bidirectional permeation of electrolytes in osmotically driven membrane processes, Environ. Sci. Technol., 45 (2011) 10642–10651.

[22] K. Lutchmiah, A.R.D. Verliefde, K. Roest, L.C. Rietveld, E.R. Cornelissen, Forward osmosis for application in wastewater treatment: a review, Water Res., 58 (2014) 179–197.

[23] Z.W. Wang, J.X. Tang, C.W. Zhu, Y. Dong, Q.Y. Wang, Z.C. Wu, Chemical cleaning protocols for thin film composite (TFC) polyamide forward osmosis membranes used for municipal wastewater treatment, J. Membr. Sci., 475 (2015) 184–192.

[24] Z.W. Wang, J.J. Zheng, J.X. Tang, X.H. Wang, Z.C. Wu, A pilot-scale forward osmosis membrane system for concentrating low-strength municipal wastewater: performance and implications, Sci. Rep., 6 (2016), https://doi.org/10.1038/srep21653.

[25] S. Phuntsho, F. Lotfi, S.K. Hong, D.L. Shaffer, M. Elimelech, H.K. Shon, Membrane scaling and flux decline during fertiliser-drawn forward osmosis desalination of brackish groundwater, Water Res., 57 (2014) 172–182.

[26] J.L. Soler-Cabezas, J.A. Mendoza-Roca, M.C. Vincent-Vela, M.J. Luján-Facundo, L. Pastor-Alcañiz, Simultaneous concentration of nutrients from anaerobically digested sludge centrate and pre-treatment of industrial effluents by forward osmosis, Sep. Purif. Technol., 193 (2018) 289–296.

[27] D.L. Shaffer, J.R. Werber, H. Jaramillo, S.H. Lin, M. Elimelech, Forward osmosis: where are we now?, Desalination, 356 (2015) 271–284.

[28] X.L. Lu, C.H. Boo, J. Ma, M. Elimelech, Bidirectional diffusion of ammonium and sodium cations in forward osmosis: role of membrane active layer surface chemistry and charge, Environ. Sci. Technol., 48 (2014) 14369–14376.

[29] N.T. Hancock, T.Y. Cath, Solute coupled diffusion in osmotically driven membrane processes, Environ. Sci. Technol., 43 (2009) 6769–6775.

[30] Y. Lei, J.C. Remmers, M. Saakes, R.D. van der Weijden, C.J.N. Buisman, Is there a precipitation sequence in municipal wastewater induced by electrolysis?, Environ. Sci. Technol., 52 (2018) 8399–8407.

Supporting information

Table S1
Supersaturation index

	CTA Membrane			TFC Membrane		
Mineral	Sat. index 0%	Sat. index 50%	Sat. index 90%	Sat. index 0%	Sat. index 50%	Sat. index 90%
Anhydrite	–2.02	–1.662	–1.451	–2.01	–1.645	–1.415
Brucite	–6.102	–3.736	–2.484	–5.036	–3.461	–2.579
$Ca_3(PO_4)_2$ (am1)	–2.322	0.055	–1.38	–2.065	–0.307	–0.533
$Ca_3(PO_4)_2$ (am2)	0.428	2.805	1.37	0.685	2.443	2.217
$Ca_3(PO_4)_2$ (beta)	1.098	3.475	2.04	1.355	3.113	2.887
$Ca_4H(PO_4)_3{:}3H_2O$(s)	0.49	3.097	0.638	0.622	2.537	2.035
$CaHPO_4$(s)	–0.362	–0.132	–1.153	–0.488	–0.329	–0.599
$CaHPO_4{:}2H_2O$(s)	–0.643	–0.413	–1.436	–0.768	–0.61	–0.884
Epsomite	–4.708	–3.902	–3.051	–4.142	–3.644	–2.856
Fluorite	–2.827	–2.472	–2.677	–2.51	–2.312	–1.706
Gypsum	–1.77	–1.413	–1.204	–1.76	–1.396	–1.171
Halite	–6.424	–5.618	–4.699	–6.624	–5.562	–4.389
Hydroxyapatite	8.325	12.849	10.999	8.966	12.321	12.138
KCl(s)	–6.543	–5.708	–4.764	–6.836	–5.358	–4.073
Lime	–21.247	–19.332	–18.725	–20.739	–19.3	–18.988
$Mg(OH)_2$ (active)	–7.796	–5.43	–4.178	–6.73	–5.155	–4.273
$Mg_2(OH)_3Cl{:}4H_2O$(s)	–13.77	–9.365	–6.655	–11.982	–8.559	–6.2
$Mg_3(PO_4)_2$(s)	–5.904	–2.176	–1.672	–3.975	–1.809	–0.316
MgF_2(s)	–5.671	–4.866	–4.424	–4.796	–4.463	–3.284
$MgHPO_4{:}3H_2O$(s)	–1.917	–1.237	–1.614	–1.485	–1.191	–0.895
Mirabilite	–6.936	–6.232	–5.219	–7.148	–6.654	–5.616
NaF(s)	–7.008	–6.656	–6.353	–6.96	–6.795	–6.076
Periclase	–10.586	–8.22	–6.967	–9.52	–7.945	–7.061
Portlandite	–11.252	–9.337	–8.731	–10.743	–9.305	–8.996
Struvite	–2.277	–0.583	–0.406	–1.706	–0.663	–0.113
Thenardite	–8.37	–7.664	–6.642	–8.582	–8.084	–7.023